

Halving warming with idealized solar geoengineering moderates key climate hazards

Peter Irvine^{1*}, Kerry Emanuel², Jie He^{3,4,5}, Larry W. Horowitz⁴, Gabriel Vecchi⁶, David Keith¹

* Contact: Peter_irvine@fas.harvard.edu

1 – John A. Paulson School of Engineering and Applied Sciences, Harvard University, Cambridge, MA, USA

2 – Lorenz Center, Massachusetts Institute of Technology, MA, USA

3 - The Program in Atmospheric and Oceanic Sciences, Princeton University, NJ, USA

4 – National Oceanic and Atmospheric Administration, Geophysical Fluid Dynamics Laboratory, Princeton, NJ, USA

5 - School of Earth and Atmospheric Sciences, Georgia Institute of Technology, GA, USA

6 - Department of Geosciences and the Princeton Environmental Institute, Princeton University, NJ, USA

Solar geoengineering (SG) could restore average surface temperatures by increasing the planetary albedo¹⁻⁴, but doing so would reduce precipitation⁵⁻⁷. Solar geoengineering might, thus, increase climate risks for some regions, even as it reduced globally-aggregated risks⁸⁻¹⁰. We analyse the fraction of locations that see local climate change exacerbated or moderated by SG. Rather than restoring temperatures, we assume that SG is applied to halve the warming produced by doubling CO₂ (half-SG). We use HiFLOR, a 25 km resolution tropical-cyclones-permitting model with a substantially improved representation of present-day precipitation extremes¹¹, and a dozen models from the Geoengineering Model Intercomparison Project (GeoMIP)¹². In HiFLOR, half-SG offsets most of the CO₂-induced increase of simulated tropical cyclone intensity, while it does not exacerbate the effect of doubling CO₂ on water availability or extreme precipitation averaged over any IPCC-SREX region; and, less than 0.4% of the land surface sees exacerbation of extreme precipitation or water availability. Concerns about the inequality of the impacts of solar geoengineering are appropriate, yet the quantitative extent of inequality may be overstated¹³. Our results suggest that no region would see aggregate impacts of climate change exacerbated by solar geoengineering that halves global temperature change.

The idea that an engineered increase in planetary albedo might offset greenhouse gas (GHG)-driven warming is more than half a century old¹. Early studies addressed the technology and its policy implications²⁻⁴, yet it was not until 2000 that a climate model was first used to study the spatial pattern of climate response to Solar Geoengineering (SG)⁷. Since then, at least 100 papers, including many from GeoMIP, have addressed the climate response to various SG scenarios^{12,14}. Some methods of SG could enable the world to keep global mean temperatures below the 1.5°C warming threshold¹⁵⁻¹⁷. But, global temperature targets are proxies for local changes in climate variables that drive impacts. SG might hypothetically reduce global mean surface temperature while still making most people worse off. Indeed, concerns about the climate's response to SG have focused on regional disparities in climate impacts and reductions in precipitation in particular^{13,18}.

The policy-relevance of prior analysis of the climate response to SG has been limited by several choices. First, many studies focused only on 2-m air temperature (T) and precipitation (P); yet without accounting for evaporation (E), precipitation alone is not an effective proxy for water

availability or agricultural productivity¹⁹. Second, many studies assumed SG was used to substitute for emission cuts by offsetting all GHG-induced warming, substantially reducing the strength of the hydrological cycle^{6,7,12}, and few existing studies evaluated scenarios where SG complements emissions reductions without offsetting all warming^{16,20}. Third, despite concern about the potential for SG to worsen climate impacts in some regions, no prior analysis has estimated the fraction of locations that see local climate change exacerbated by SG, where “exacerbated” means that the absolute deviation from control is increased by SG.

We analyse the distribution of climate changes resulting from reducing the solar constant to offset roughly half the radiative forcing from doubling CO₂. A spatially uniform reflective stratospheric aerosol layer, which could be achieved by adjusting aerosol injection using feedback^{21,22}, would produce a similar radiative forcing to a solar constant reduction. Even with a uniform distribution, stratospheric sulphate SG will differ from a solar constant reduction in that sulphates heat the lower stratosphere, perturb the ozone layer, and increase the ratio of diffuse to direct light¹⁵. Each of these effects can be reduced by choices of alternate non-sulphate aerosol, though their side-effects are less well understood because there is no direct natural analogue²³. We nevertheless choose solar constant reduction as a benchmark because, given the diverse implementations of aerosols in models, solar modification allows more direct tests of inter-model differences in climate response to SG.

We use the GFDL HiFLOR model run at a horizontal resolution of ~25 km (see Methods)^{11,24,25}. The model endogenously generates tropical cyclones with up to Category 5 intensity and significantly reduces biases in regional temperature and precipitation extremes of the current climate compared to lower resolution versions of its model family^{11,24}. Relative to a present-day control experiment, we compare the climate response over a 100-year period of an experiment in which CO₂ is doubled (2xCO₂ experiment) to that of an experiment in which the solar constant is reduced by 1% to approximately offset half of the warming from the CO₂ doubling (half-SG experiment, see Methods). We test the robustness of the HiFLOR results by comparing them to those of 12 climate models that participated in the GeoMIP G1 experiment^{12,26}, in which the global mean temperature response to an instantaneous quadrupling of CO₂ concentrations is fully offset using a model-dependent reduction in solar constant of roughly 4%. We generate a synthetic half-SG scenario for each of the GeoMIP models by linearly scaling all variables to a value midway between their G1 and 4xCO₂ values (see Methods).

We analysed annual means of T, P - E (PE), yearly maximum temperature (Tx), yearly maximum precipitation in a 5-day window (Px), and the power dissipation index (PDI) of tropical cyclones (see Methods)²⁷. These five variables span most of the drivers of the “key risks of climate change” identified by the IPCC with the notable exception of sea-level rise (Extended Data Table 1). In contrast to much of the prior literature on solar geoengineering, we exclude annual-mean P as it is a less effective proxy for water availability than PE¹⁹, and a less effective proxy for flood risk than Px²⁸ (though results are included in Extended Data).

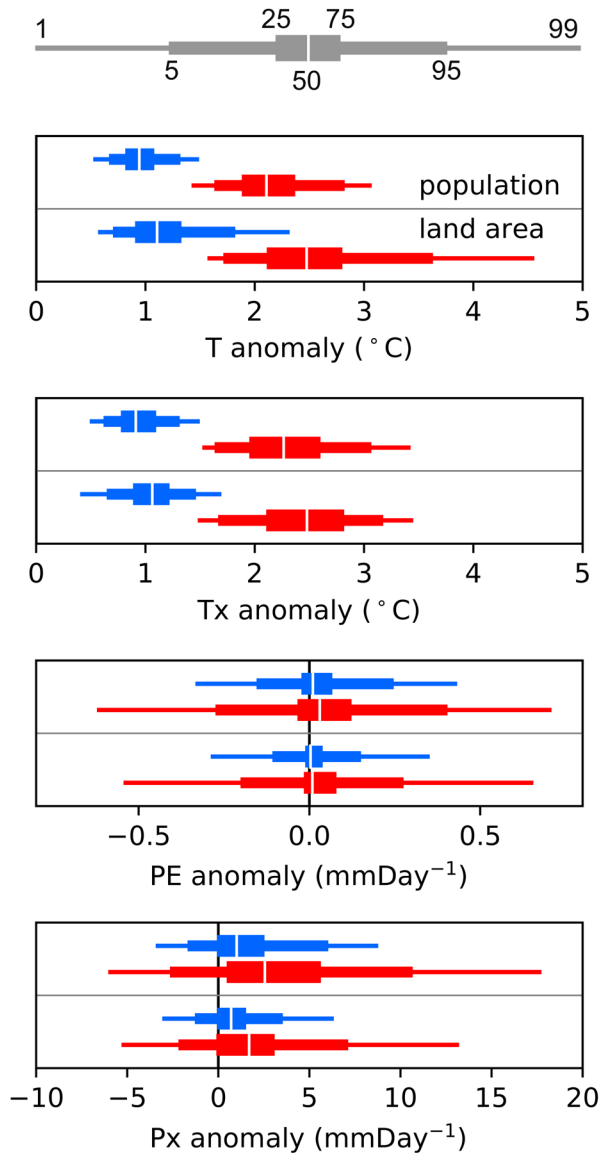


Figure 1. The distribution of $2\times\text{CO}_2$ and half-SG anomalies by land area and population. The distribution of $2\times\text{CO}_2$ (red) and half-SG (blue) anomalies versus control for the HiFLOR model are plotted by land area (bottom), excluding Greenland and Antarctica, and by population (top) for, from top to bottom, surface air temperature (T), maximum annual T (Tx), precipitation – evaporation (PE), maximum annual 5-day precipitation (Px) (see Methods). The legend above illustrates how the percentiles of the distribution are shown.

Figure 1 shows the distribution of climate changes under $2\times\text{CO}_2$ and half-SG versus the control. Since we are focusing on changes relevant to human and terrestrial ecological impacts, we examine land only, excluding Greenland and Antarctica, and compare area-weighted and population-weighted results. It is well known that SG suppresses the hydrological cycle and previous work suggested SG causes drying^{5,18,26}. The half-SG scenario reduces the global average P increase from 3.0 % under $2\times\text{CO}_2$ to 0.5% under half-SG. Perhaps surprisingly, half-SG also reduces the fraction of land surface that sees drying as measured by a decrease in PE. Under $2\times\text{CO}_2$, 3.7% of land surface sees a reduction of PE by more than 0.25 mm day^{-1} , whereas only 1.4% see the same drying under half-SG. The substantial reduction in the magnitude of both positive and negative anomalies shown in Figure

1 holds for the synthetic half-SG GeoMIP results, for percentage change and standard deviation normalized anomalies, and for precipitation (Extended Data Figures 1-3).

	Fraction Exacerbated				Fraction Moderated			
	HiFLOR	GeoMIP			HiFLOR	GeoMIP		
		Med	Min	Max		Med	Min	Max
T	0.0 %	0.0 %	0.0 %	0.0 %	100.0 %	100.0 %	99.2 %	100.0 %
Tx	0.0 %	0.0 %	0.0 %	0.3 %	100.0 %	100.0 %	98.9 %	100.0 %
PE	0.4 %	1.9 %	0.3 %	4.8 %	26.4 %	29.6 %	22.3 %	65.9 %
Px	0.4 %	0.8 %	0.1 %	7.3 %	41.6 %	44.9 %	28.2 %	60.9 %

Table 1. The fraction of the land surface that sees the effects of 2xCO₂ (relative to control) significantly exacerbated or moderated by half-SG. The percentage of the land area (excluding Greenland and Antarctica) experiencing a statistically significantly greater (exacerbated) or lesser (moderated) absolute magnitude of anomaly for half-SG compared to 2xCO₂ (see Methods). Median, minimum and maximum for GeoMIP are calculated across the ensemble of individual model results.

Which regions are made worse off? Half-SG reduces the fraction of land area experiencing extreme climatic changes (Figure 1), but that does not tell us what fraction of points see their climate made worse. To test this, we define the effects of climate change as exacerbated if the absolute magnitude of the half-SG anomaly from the control is significantly greater than the 2xCO₂ anomaly, and that they are moderated if half-SG significantly reduces the absolute magnitude of the anomaly. If the control climate is assumed to be preferable to a disturbed climate, then exacerbated/moderated implies that the region is worse/better off. But, this will not always be true as some communities may prefer the altered climate. Table 1 shows the fraction of the land surface where half-SG exacerbates or moderates the effects of 2xCO₂ computed using a set of 90% *t*-tests applied to the values at each grid-point (see Methods). T and Tx changes are moderated over almost the entire land surface across all models. For PE and Px, the area moderated is far greater than the area exacerbated in the HiFLOR model and the GeoMIP ensemble. But note that many points do not show a significant change (do not pass the *t*-test). Results are similar when weighted by population and if calculated on a seasonal basis, though the fraction exacerbated in HiFLOR is somewhat greater for PE and Px at ~1 % (Extended Data Tables 2 and 3).

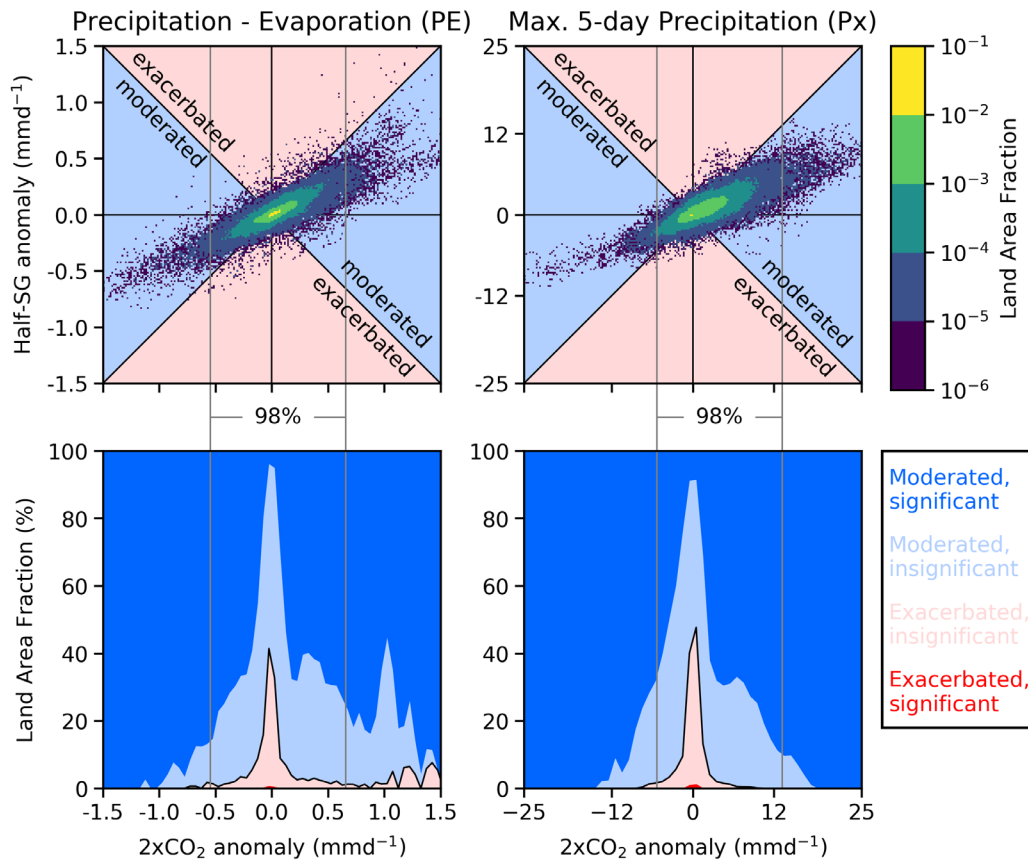


Figure 2. The joint distribution of $2xCO_2$ and half-SG anomalies with results for the fraction of the land surface where half-SG exacerbates or moderates the climate trend. Top, 2D-histograms show the distribution across the land area, excluding Greenland and Antarctica, of the $2xCO_2$ and half-SG anomalies versus control in precipitation minus evaporation (PE, left) and maximum 5-day precipitation (Px, right). To generate the bins for the 2D-histogram, the X and Y axes are divided into 200 intervals. The fraction of the land area with anomalies that fall into each bin are indicated by the colour scale, empty bins are not plotted. All points falling closer to the x-axis than the diagonal 1:1 lines see the magnitude of the trend reduced (moderated, blue background) by half-SG and all those above and below these lines see the magnitude of the trend increased (exacerbated, pink background). Note all points, including those that don't see significant change are plotted. Bottom, the fraction of the area in which the impacts of $2xCO_2$ are exacerbated (red) or moderated (blue) by half-SG as a function of the $2xCO_2$ anomaly. Bold colours indicate statistically significant results and pale colours indicate insignificant results.

Figure 2 compares $2xCO_2$ and half-SG anomalies (relative to control) of all land points and shows the fraction of points that are exacerbated or moderated as a function of the $2xCO_2$ anomaly. Since points with no change under $2xCO_2$ cannot see that change reduced, the fraction moderated tends to zero as the $2xCO_2$ anomaly tends to zero. Points with large anomalies under $2xCO_2$ are almost all moderated, while the points that are exacerbated almost all experience very small climatic change, i.e., those regions experiencing the greatest climate change are most likely to see it reduced by half-

SG. Similar results are found for precipitation, while temperature is significantly reduced at all locations (Extended Data Fig 4).

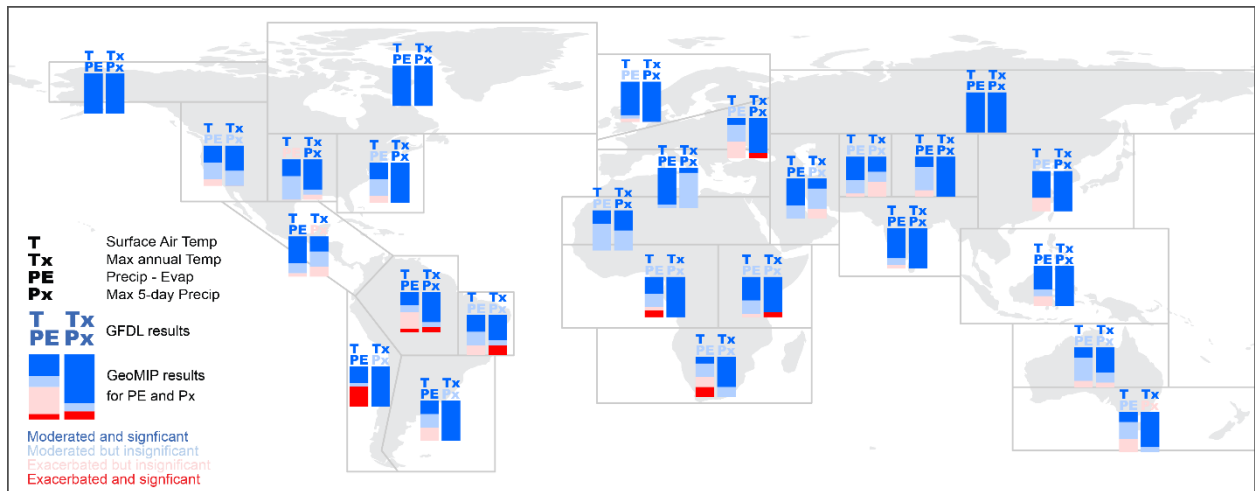


Figure 3. Regional distribution of where half-SG moderates or exacerbates the absolute magnitude of $2xCO_2$ anomalies in HiFLOR (for T, Tx, PE, and Px) and the GeoMIP ensemble (PE and Px). Regions where half-SG moderates (blue) or exacerbates (red) the absolute magnitude of the $2xCO_2$ climate anomalies relative to control are illustrated. Statistically significant results are indicated with bold colours whereas insignificant results are shown with pale colours (see Methods). The results for the GeoMIP models are shown for PE (left-column) and Px (right-column) with the columns coloured to indicate the fraction of GeoMIP models with each result. All GeoMIP models show a statistically significant reduction in T and Tx in all regions (not shown). Note, all model-regions which show a statistically significantly greater change for half-SG see greater PE in half-SG than in $2xCO_2$ or the control, and less Px in half-SG than in $2xCO_2$ or the control.

Only the strongest climate trends are detectable at small spatial scales; to test for weaker, larger-scale trends we aggregate results to the representative climate regions used in the IPCC Special Report on Extremes (SREX, see Methods). Figure 3 provides a global overview of the effects of SG on the climate variables assessed here, allowing a qualitative evaluation of whether a region would expect to see aggregate climate risks moderated or exacerbated under half-SG compared to $2xCO_2$. None of the four variables are exacerbated (under a 90% *t*-test) by half-SG in the HiFLOR model in any region. A few regions show PE or Px exacerbated in at least one GeoMIP model, though in only Western South America and South Africa for PE do the number of models showing an exacerbation exceed the number showing a moderation.

Note, however that in the model regions where half-SG exacerbates change, all had a larger PE in half-SG than either $2xCO_2$ or control. So, in the few regions where half-SG exacerbates climate change, it increases water availability. This stands in contrast to previous studies and commentary which highlighted concerns that SG would lead to drought^{6,10,18}. For Px, in all model regions where half-SG exacerbates change, there is less extreme precipitation than in either $2xCO_2$ or control, indicating less risk of flooding.

Finally, we examined the global intensity of tropical cyclones, including hurricanes and typhoons; directly simulating tropical cyclone response to solar geoengineering in a global model for the first time^{29,30}. $2xCO_2$ increases the sum of the power dissipation index over all tropical cyclones in HiFLOR by 17.6% compared to the control. Half-SG offsets most of this, reducing the increase in PDI to 2.4%.

As there is presently substantial uncertainty in regional projections of TC activity changes^{31,32}, in this paper we provide only the global results. In addition, we downscaled the HiFLOR output using the technique of Emanuel et al. (2008)³¹ to produce 40,000 synthetic cyclones globally in years 100-300 of the control and 2xCO₂ climates, and 26,000 events in years 171-300 of the half-SG climate (see Methods). The downscaled storms show a much weaker response than HiFLOR, with a 5.1% increase in PDI in 2xCO₂ and a 2.0% decrease in half-SG, both relative to the control. This result differs substantially from downscaling CMIP5 models for emissions pathway RCP 8.5³³, which showed large increases in power dissipation. We speculate that well-resolved tropical cyclones in the fully coupled HiFLOR model may retard changes in monthly mean potential intensity³⁴, damping the response of synthetic storms to climate change.

We focused on an idealized SG scenario that approximately halves the warming from doubling CO₂, and so more-or-less restores the intensity of the hydrological cycle, rather than the typical scenario in which SG offsets all warming. Extended Data Figure 5 shows how the outcomes change as a function of the level of solar constant reduction and makes clear that beyond offsetting around half of the warming from 2xCO₂, the marginal benefits of further cooling decline and the fraction of the land in which climate change is exacerbated grows. While we do not claim that halving warming is necessarily optimal, we suggest it is a better starting point for analysis than a complete offset scenario, as it avoids more-than-reversing many climate trends as happens under scenarios which offset all warming.

It would be premature to conclude from this study that no region would experience greater aggregate climate risks in a real-world deployment of SG that halved anthropogenic warming, as we analysed an idealized scenario and a limited set of climate variables. Our results do not, however, support the common claims that SG would inevitably lead to significant harms to some regions¹⁸, nor the claims that SG's benefits and harms always have a strongly unequal distribution¹³.

Acknowledgements

We acknowledge the World Climate Research Programme's Working Group on Coupled Modelling, which is responsible for CMIP, and we thank the climate modeling groups for producing and making available their model output. For CMIP the U.S. Department of Energy's Program for Climate Model Diagnosis and Intercomparison provides coordinating support and led development of software infrastructure in partnership with the Global Organization for Earth System Science Portals. We thank all participants of the Geoengineering Model Intercomparison Project and their model development teams, CLIVAR/WCRP Working Group on Coupled Modeling for endorsing GeoMIP, and the scientists managing the Earth System Grid data nodes who have assisted with making GeoMIP output available. The authors acknowledge the help of Charles Curry who provided the extreme indices data for the GeoMIP ensemble. The authors acknowledge Robert Stanhope for help finalizing the figures. The authors would like to thank David Fahey and Ken Caldeira for comments on the draft and Lee Miller, Gernot Wagner and Daniel Kluger for helpful discussions on the statistical approach.

References

1. PSAC *et al.* *Restoring the quality of our environment*. (President's Science Advisory Committee, 1965).
2. Keith, D. W. & Dowlatabadi, H. A serious look at geoengineering. *Eos* **73**, 289–292 (1992).
3. Schelling, T. C. Climatic Change: Implications for Welfare and Policy. in *Changing Climate* (eds. Nierenberg, W. A. et al.) (National Academy of Sciences, 1983).
4. Teller, E., Wood, L. & Hyde, R. Global warming and ice ages: I. Prospects for physics-based modulation of global change. (1997).
5. Tilmes, S. *et al.* The hydrological impact of geoengineering in the Geoengineering Model Intercomparison Project (GeoMIP). *J. Geophys. Res. Atmospheres* **118**, 11036–11058 (2013).
6. Lunt, D. J., Ridgwell, A., Valdes, P. J. & Seale, A. 'Sunshade World': A fully coupled GCM evaluation of the climatic impacts of geoengineering. *Geophys. Res. Lett.* **35**, L12710 (2008).
7. Govindasamy, B. & Caldeira, K. Geoengineering Earth's radiation balance to mitigate CO₂-induced climate change. *Geophys. Res. Lett.* **27**, 2141–2144 (2000).
8. Irvine, P. J., Ridgwell, A. J. & Lunt, D. J. Assessing the regional disparities in geoengineering impacts. *Geophys. Res. Lett.* **37**, (2010).
9. Ricke, K. L., Moreno-Cruz, J. B. & Caldeira, K. Strategic incentives for climate geoengineering coalitions to exclude broad participation. *Environ. Res. Lett.* **8**, 014021 (2013).
10. Crook, J., Jackson, L. S., Osprey, S. M. & Forster, P. M. A Comparison of Temperature and Precipitation Responses to Different Earth Radiation Management Geoengineering Schemes. *J. Geophys. Res. Atmospheres* **120**, 9352–9373 (2015).
11. van der Wiel, K. *et al.* The Resolution Dependence of Contiguous U.S. Precipitation Extremes in Response to CO₂ Forcing. *J. Clim.* **29**, 7991–8012 (2016).
12. Kravitz, B. *et al.* The Geoengineering Model Intercomparison Project (GeoMIP). *Atmospheric Sci. Lett.* **12**, 162–167 (2011).

13. National Research Council. *Climate Intervention: Reflecting Sunlight to Cool Earth*. (National Academies Press, 2015).
14. Irvine, P. J., Kravitz, B., Lawrence, M. G. & Muri, H. An overview of the Earth system science of solar geoengineering. *Wiley Interdiscip. Rev. Clim. Change* n/a-n/a (2016). doi:10.1002/wcc.423
15. Boucher, O. *et al.* Clouds and Aerosols. in *Climate Change 2013: The Physical Science Basis. Contribution of Working Group I to the Fifth Assessment Report of the Intergovernmental Panel on Climate Change* (eds. Stocker, T. F. *et al.*) (Cambridge University Press, 2013).
16. MacMartin, D. G., Ricke, K. L. & Keith, D. W. Solar geoengineering as part of an overall strategy for meeting the 1.5°C Paris target. *Phil Trans R Soc A* **376**, 20160454 (2018).
17. Jones, A. C. *et al.* Regional Climate Impacts of Stabilizing Global Warming at 1.5 K Using Solar Geoengineering. *Earths Future* **6**, 230–251 (2018).
18. Robock, A., Oman, L. & Stenchikov, G. L. Regional climate responses to geoengineering with tropical and Arctic SO₂ injections. *J. Geophys. Res.-Atmospheres* **113**, D16101 (2008).
19. Swann, A. L. S., Hoffman, F. M., Koven, C. D. & Randerson, J. T. Plant responses to increasing CO₂ reduce estimates of climate impacts on drought severity. *Proc. Natl. Acad. Sci.* **113**, 10019–10024 (2016).
20. MacMartin, D. G., Caldeira, K. & Keith, D. W. Solar geoengineering to limit the rate of temperature change. *Philos. Trans. R. Soc. Math. Phys. Eng. Sci.* **372**, (2014).
21. Dai Z., Weisenstein D. K. & Keith D. W. Tailoring Meridional and Seasonal Radiative Forcing by Sulfate Aerosol Solar Geoengineering. *Geophys. Res. Lett.* **45**, 1030–1039 (2018).
22. Kravitz Ben *et al.* First Simulations of Designing Stratospheric Sulfate Aerosol Geoengineering to Meet Multiple Simultaneous Climate Objectives. *J. Geophys. Res. Atmospheres* **122**, 12,616-12,634 (2018).
23. Keith, D. W., Weisenstein, D. K., Dykema, J. A. & Keutsch, F. N. Stratospheric solar geoengineering without ozone loss. *Proc. Natl. Acad. Sci.* **113**, 14910–14914 (2016).

24. Murakami, H. *et al.* Simulation and Prediction of Category 4 and 5 Hurricanes in the High-Resolution GFDL HiFLOR Coupled Climate Model. *J. Clim.* **28**, 9058–9079 (2015).
25. Bhatia, K., Vecchi, G. A., Murakami, H., Underwood, S. D. & Kossin, J. Projected Response of Tropical Cyclone Intensity and Intensification in a Global Climate Model - SUBMITTED. *J. Clim.* (2018).
26. Kravitz, B. *et al.* Climate model response from the Geoengineering Model Intercomparison Project (GeoMIP). *J. Geophys. Res. Atmospheres* **118**, 8320–8332 (2013).
27. Emanuel, K. Increasing destructiveness of tropical cyclones over the past 30 years. *Nature* **436**, 686–688 (2005).
28. Curry, C. L. *et al.* A multi-model examination of climate extremes in an idealized geoengineering experiment. *J. Geophys. Res. Atmospheres* **119**, 3900–3923 (2014).
29. Jones, A. C. *et al.* Impacts of hemispheric solar geoengineering on tropical cyclone frequency. *Nat. Commun.* **8**, 1382 (2017).
30. Wang, Q., Moore, J. C. & Ji, D. A statistical examination of the effects of stratospheric sulfate geoengineering on tropical storm genesis. *Atmospheric Chem. Phys.* **18**, 9173–9188 (2018).
31. Emanuel, K., Sundararajan, R. & Williams, J. Hurricanes and Global Warming: Results from Downscaling IPCC AR4 Simulations. *Bull. Am. Meteorol. Soc.* **89**, 347–368 (2008).
32. Walsh, K. J. E. *et al.* Tropical cyclones and climate change. *Wiley Interdiscip. Rev. Clim. Change* **7**, 65–89 (2016).
33. Emanuel, K. A. Downscaling CMIP5 climate models shows increased tropical cyclone activity over the 21st century. *Proc. Natl. Acad. Sci.* **110**, 12219–12224 (2013).
34. Emanuel, K. A simple model of multiple climate regimes. *J. Geophys. Res. Atmospheres* **107**, ACL 4-1-ACL 4-10 (2002).